Electronic Supplementary Material (ESI) for Nanoscale.

Supporting Materials

Improved Efficiency and Thermal Stability of Ternary All-Small-Molecule Organic Solar Cells by NCBA as a Third Component Material

Zhiyong Liu[a*] and Ning Wang[b*]

[a]College of Science, Shenyang Agricultural University, Shenyang 110866, People's Republic of China

[b]Key Laboratory of Physics and Technology for Advanced Batteries (Ministry of Education), College of Physics, Jilin University, Changchun 130012, China

[*]Corresponding authors: (zhyliu2006@hotmail.com (Z.Y. Liu); ningwang@jlu.edu.cn (N. Wang))

2. Experimental details

2.1 Materials

p-DTS-($FBTTh_2$)$_2$ was purchased from 1-Material Inc. NCBA and $PC_{71}BM$ was purchased from Luminescence Technology Co; *o*-dichlor-obenzene (ODCB) and 1,8-diiodooctane (DIO) were purchased from Sigma-Aldrich Co. MoO_3 and Ag were purchased from Alfa Aesar Co. A mixture of *p*-DTS-($FBTTh_2$)$_2$ and blend acceptor was dissolved in ODCB solvent (3:2) with stirring overnight, and then diluted to 25 mg mL^{-1} in total without stirring and kept for over 3 h. ZnO solution was synthesized by sol-gel method [1, 2].

2.2 Device preparation and characteristics

The ITO glasses were pre-cleaned by ultrasonic bath and UV ozone treat in a plasma asher (100 W, 20 min). A thin layer (20 nm) of ZnO was spin-coated onto the ITO glass and baked at 150 ^{O}C for 20 min in air. A blend solution of *p*-DTS-($FBTTh_2$)$_2$, NCBA and $PC_{71}BM$ was spin-coated on the ZnO layer to form an photoactive layer and thermal annealing treatment were carried out in a N_2-filled glove box and the nominal thickness of ~100 nm (with a variation of ~15 nm over the entire film). A MoO_3 layer and Ag electrode were evaporated under vacuum through a shadow mask to define the active area of the devices (3×3 mm^2). The current density versus voltage (*J–V*) characteristics of PSCs were performed in a glove box with a computer-controlled Keithley 236 Source Measure Unit under illumination at 100 mW cm^{-2} using an AM1.5 G solar simulator. The external quantum efficiency (*EQE*) spectrum was measured with the Stanford Research Systems model SR830 DSP lock-in amplifier coupled with a

WDG3 monochromator and a 500 W xenon lamp.

The hole-only space-charge-limited-current (SCLC) devices and electron-only SCLC devices were fabricated with structures of ITO/PEDOT:PSS/PBDB-T:ITIC:F-N2200/Au and Al/PBDB-T:ITIC:F-N2200/Al, respectively. The charge carrier mobilities were calculated using the equation [3, 4]:

$$J = \frac{9}{8}\varepsilon_r\varepsilon_0\mu\frac{V^2}{d^3},$$

where J is the current density, μ is the charge carrier mobility, ε_0 ($8.85\times10_{-14}$ F/cm) and ε_r the permittivity of free space and relative permittivity of the material (ε_r was assumed to be 3), respectively, and V is the SCLC effective voltage. The charge carrier mobility were calculated using the equation [5]:

$$\mu = \mu_0 \exp[0.89\gamma\sqrt{\frac{V}{L}}]$$

where μ_0 is the charge mobility under zero electric field and γ is a constant. Then, the Mott-Gurney equation can be described by [6]:

$$J = \frac{9}{8}\varepsilon_r\varepsilon_0\mu_0\frac{V^2}{L^3}\exp[0.89\gamma\sqrt{\frac{V}{L}}]$$

In this case, the charge mobility were estimated using the following equation [6]:

$$\ln(\frac{JL^3}{V^2}) = 0.89\gamma\sqrt{\frac{V}{L}} + \ln(\frac{9}{8}\varepsilon_r\varepsilon_0\mu_0)$$

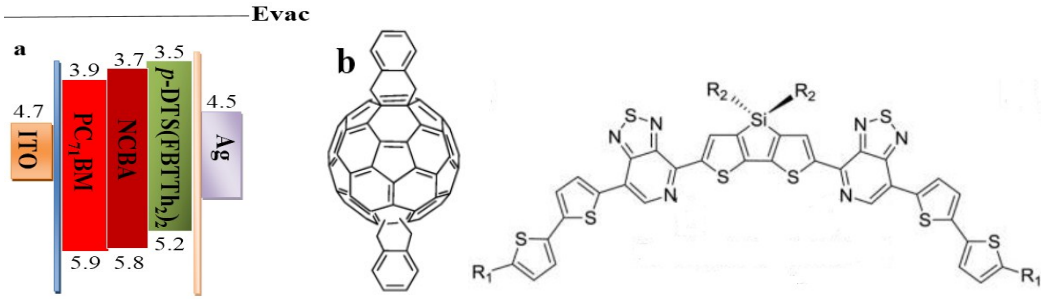

Figure S1. Energy band diagram of the ternary OSC for figure (a) and the chemical structure of NCBA and *p*-DTS-$(FBTTh_2)_2$ for figure (b).

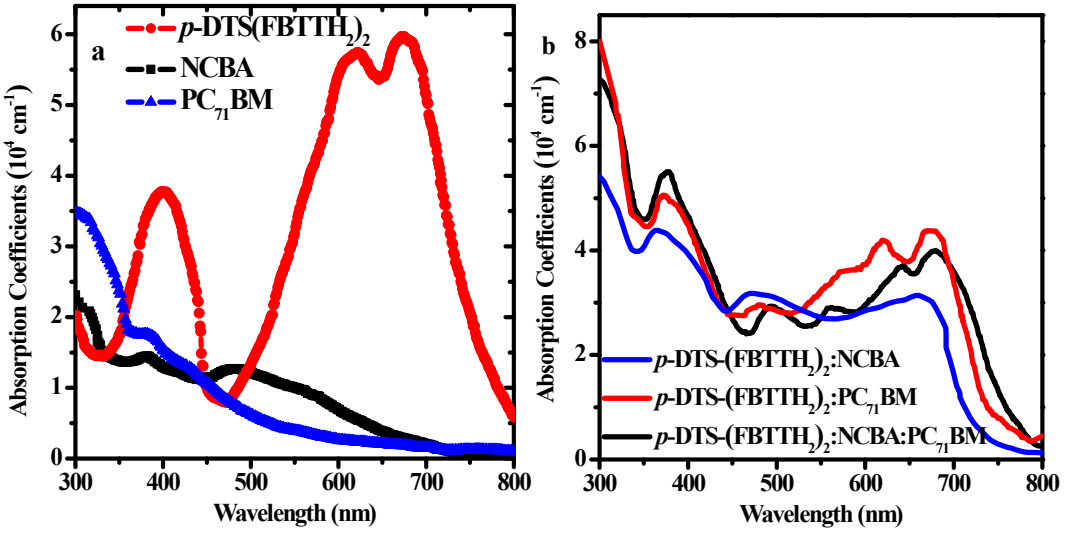

Figure S2. (a) Absorption spectra of neat *p*-DTS-$(FBTTh_2)_2$, NCBA, and $PC_{71}BM$, and (b) binary thin films of *p*-DTS-$(FBTTh_2)_2$:$PC_{71}BM$ and *p*-DTS-$(FBTTh_2)_2$:NCBA and ternary thin films of *p*-DTS-$(FBTTh_2)_2$:NCBA:$PC_{71}BM$ (3:0.24:1.76).

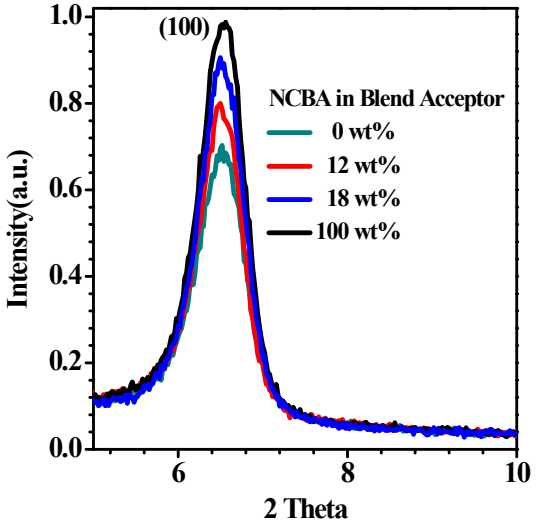

Figure S3. XRD patterns of *p*-DTS-$(FBTTh_2)_2$:NCBA:$PC_{71}BM$ ternary thin films with NCBA concentrations in the blend acceptor of 0, 12, 18, and 100 wt.%.

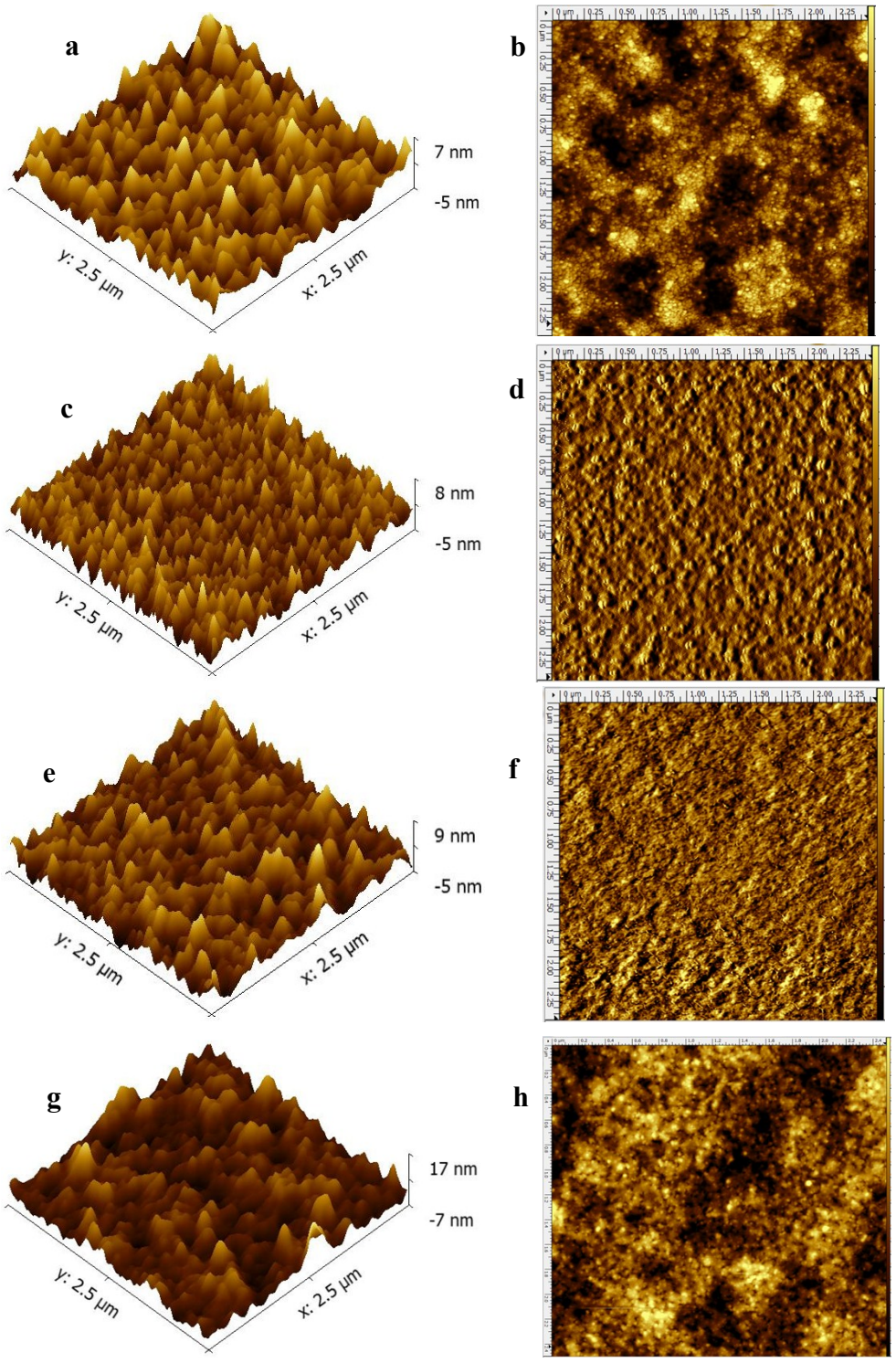

Figure S4. 3D and phase images of AFM images of the binary and ternary thin films. *p*-DTS-$(FBTTh_2)_2$:$PC_{71}BM$=3:2 for (a and b); (b) *p*-DTS-

$(FBTTh_2)_2$:NCBA:$PC_{71}BM$=3:0.24:1.76 for (c and d); (c) *p*-DTS-$(FBTTh_2)_2$:NCBA:$PC_{71}BM$=3:0.36:1.64 for (e and f); (d) *p*-DTS-$(FBTTh_2)_2$:NCBA=3:2 for (g and h).

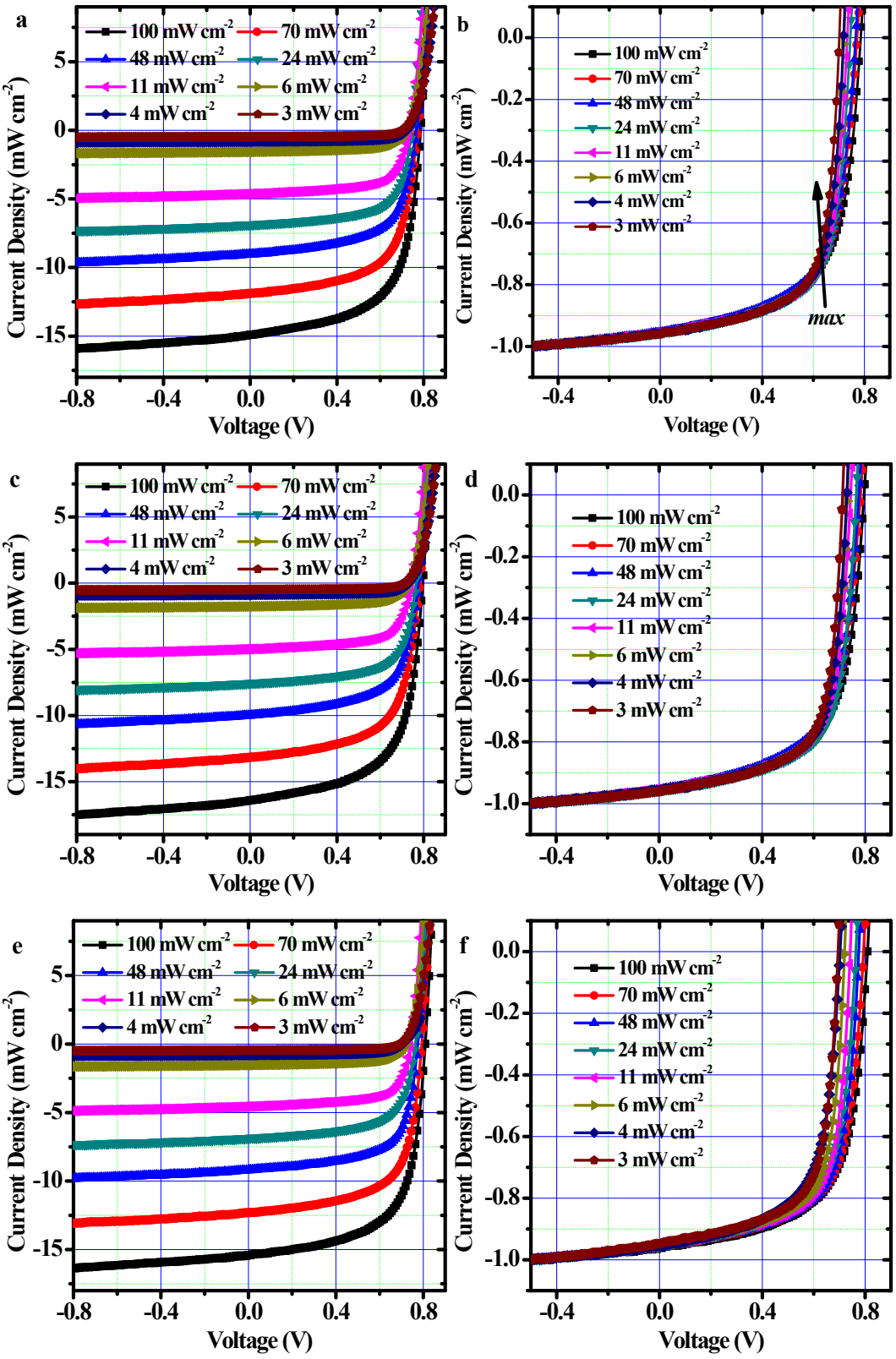

Figure S5. (a, c, and e) Current-voltage characteristics of binary *p*-DTS-(FBTTh$_2$)$_2$:PC$_{71}$BM- and ternary *p*-DTS-(FBTTh$_2$)$_2$:NCBA:PC$_{71}$BM (3:0.24:1.76) and *p*-DTS-(FBTTh$_2$)$_2$:NCBA:PC$_{71}$BM (3:0.36:1.64)-based OSCs dependent on incident light intensity; (b, d and f) normalized photocurrents at −0.5 V measured for various intensities.

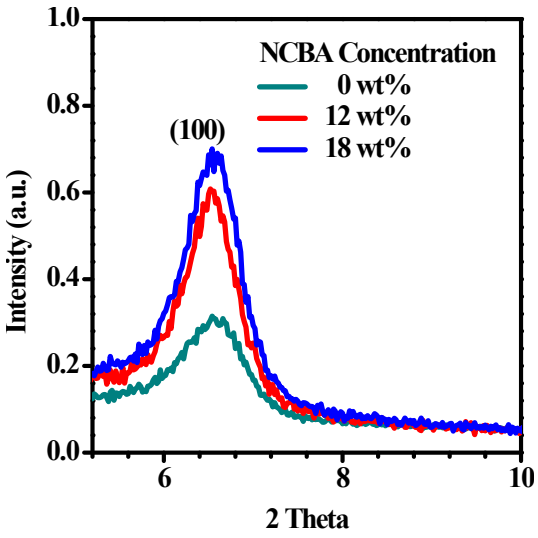

Figure S6. XRD curves of binary *p*-DTS-(FBTTh$_2$)$_2$:PC$_{71}$BM, ternary *p*-DTS-(FBTTh$_2$)$_2$:NCBA:PC$_{71}$BM (3:0.24:1.76), and ternary *p*-DTS-(FBTTh$_2$)$_2$:NCBA:PC$_{71}$BM (3:0.36:1.64) thin films after 100 h of thermal annealing treatment at 90°C.

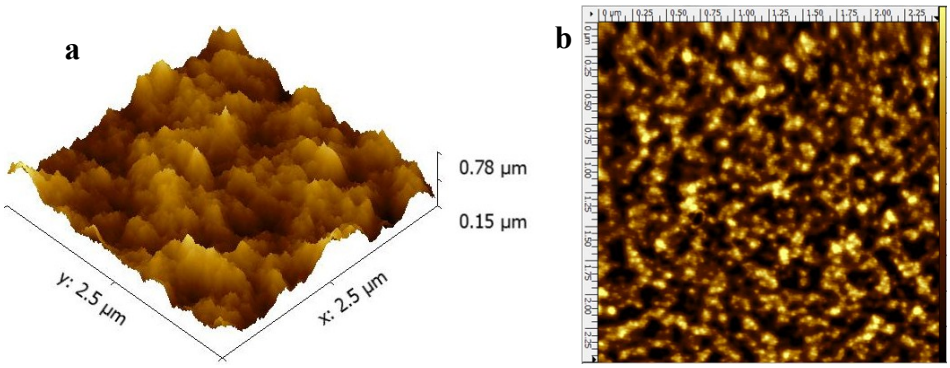

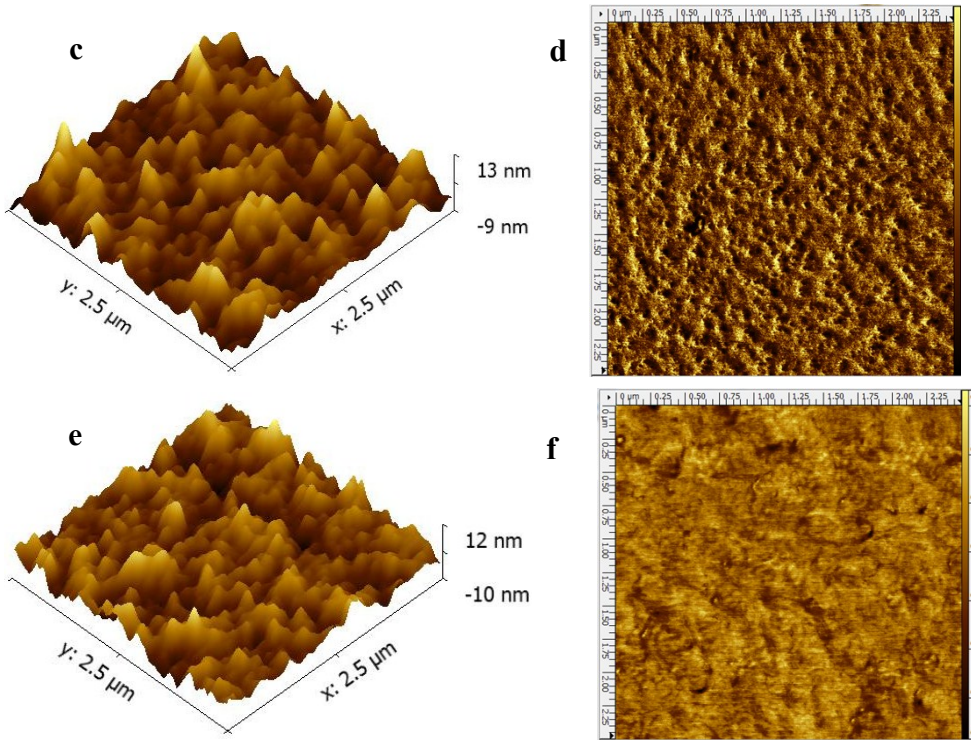

Figure S7. 3D and phase images of AFM images of binary *p*-DTS-$(FBTTh_2)_2$:$PC_{71}BM$ for (a and b), ternary *p*-DTS-$(FBTTh_2)_2$:NCBA:$PC_{71}BM$ (3:0.24:1.76) for (c and d), and ternary *p*-DTS-$(FBTTh_2)_2$:NCBA:$PC_{71}BM$ (3:0.36:1.64) thin films for (e and f) after 100 h of thermal annealing treatment at 90°C.

Reference:

1. W. Yu, L. Huang, D. Yang, P. Fu, L. Zhou, J. Zhang and C. Li, *Journal of Materials Chemistry A*, 2015, **3**, 10660-10665.
2. U. Galan, Y. Lin, G. J. Ehlert and H. A. Sodano, *Composites Science and Technology*, 2011, **71**, 946-954.
3. H.-W. Li, Z. Guan, Y. Cheng, T. Lui, Q. Yang, C.-S. Lee, S. Chen and S.-W. Tsang, *Advanced Electronic Materials*, 2016, **2**, 1600200-1600209.
4. V. Narasimhan, D. Jiang and S.-Y. Park, *Applied Energy*, 2016, **162**, 450-459.
5. Q. An, F. Zhang, Q. Sun, M. Zhang, J. Zhang, W. Tang, X. Yin and Z. Deng, *Nano Energy*, 2016, **26**, 180-191.
6. Q. An, F. Zhang, W. Gao, Q. Sun, M. Zhang, C. Yang and J. Zhang, *Nano Energy*, 2018, **45**, 177-183.